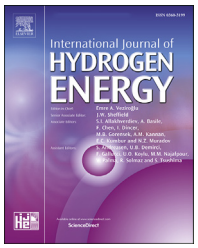
Available online at www.sciencedirect.com

ScienceDirect

journal homepage: www.elsevier.com/locate/he



Carbon nanotube (CNT) modified carbon fiber/epoxy composite plates for the PEM fuel cell bipolar plate application

Fatih Darıcık [a,*], *Alparslan Topcu* [a,b], *Kadir Aydın* [b], *Selahattin Çelik* [c]

[a] *Alanya Alaaddin Keykubat University, Rafet Kayış Faculty of Engineering, Department of Mechanical Engineering, Antalya, 07425, Turkey*

[b] *Çukurova University, Faculty of Engineering, Department of Automotive Engineering, Adana, 01330, Turkey*

[c] *Ankara Yıldırım Beyazıt University, Department of Mechanical Engineering, 06010, Ankara, Turkey*

HIGHLIGHTS

- 120 S/cm electrical conductivity was achieved with the 1.25% CNT reinforcement.
- CNTs can increase the flexural strength of the BP up to 42%.
- CNTs can increase the flexural modulus of the BP up to 27%.
- CNT-modified BP was executed pretty close performance compared to the AA 3105.

ARTICLE INFO

Article history:
Received 17 June 2022
Received in revised form
8 September 2022
Accepted 29 September 2022
Available online 22 October 2022

Keywords:
PEM fuel cell
Composite
Bipolar plate
MWCNT
Flexural
Performance tests

ABSTRACT

Light structures of the composite materials are prominent outcomes for reducing the total stack weight. However, the poor electrical properties of the composite structures pose an obstacle to wide employment as a bipolar plate for the PEMFC systems. In the current study, the carbon fiber/epoxy composite laminates were modified with the multi-walled carbon nanotube superconductor materials to overcome conductivity issues. The effects of CNTs additives in a range of 0.25–1.25% wt on the electrical, mechanical, and performance features of the carbon fiber/epoxy laminates were investigated. Electrical conductivities of the nonconductive carbon fiber/epoxy plates increased with the rising additive ratio, as expected, and reached 120 S/cm for the 1.25% CNT reinforcement. Although the mechanical strength of the pristine composite BP is already satisfactory, CNTs can increase the flexural strength and flexural modulus of the BP up to 42% and 27%, respectively. Each composite plate was subjected to the single-cell performance test. 1.25% wt CNT modified plate was executed pretty close performance compared to the aluminum alloy (AA 3105) bipolar plate under the same conditions.

© 2022 Hydrogen Energy Publications LLC. Published by Elsevier Ltd. All rights reserved.

* *Corresponding author.*
E-mail addresses: fatih.daricik@alanya.edu.tr (F. Darıcık), alparslan.topcu@alanya.edu.tr (A. Topcu), kdraydin@gmail.com (K. Aydın), selahattincelik@aybu.edu.tr (S. Çelik).

https://doi.org/10.1016/j.ijhydene.2022.09.297

0360-3199/© 2022 Hydrogen Energy Publications LLC. Published by Elsevier Ltd. All rights reserved.

Introduction

Fuel cells offer energy conversion systems that have high power density, silent operation, and zero-emission features [1]. Among fuel cell types, PEM (proton exchange membrane or polymer electrolyte) fuel cell comes forward as the most developed fuel cell type and it is commercially used in automotive and aviation applications today [2]. Intensive efforts are being made to commercialize existing prototype applications in various industries such as transportation [3], military [4], portable [5], and submarines [6]. In addition, the PEM fuel cells powered unmanned aerial vehicles (UAVs) can extend the flight time compared to the battery-electric system with the same weight [7]. Moreover, rapid refueling is another virtue of the fuel cell system [8]. Thereby, the breakthrough in the weight reduction of the stack will be contributed to extend the driving time.

Bipolar plate (BP) is one of the key components of the PEMFC system which separates and distributes reactant and oxidant gases thanks to its channel system and collecting current in the cell [9]. BPs should have high electrical conductivity, high mechanical strength, high corrosion resistance, low gas permeability, low cost, and easy machinability characteristics [10]. Also, BPs possess ~70% of stack weight and ~25% of stack cost [11,12].

Graphite materials are the most widely used BPs due to their superior electrical conductivity (10^4 S/cm at room temperature). Besides their good electrical conductivity, graphite BPs have some disadvantages, such as brittleness, and high cost [13]. Metallic BPs also present good performance with their robust structure and good conductivity. But humid nature of the fuel cell stacks causes easy corrosion and deterioration of the metallic BPs [14]. For this reason, alternative materials are investigated to be used as BP instead of graphite materials for many years. Composite materials, stainless steel materials, and alloys are the most considered materials for BP application. Polymer matrix composite materials have high mechanical strength as well as lightweight structures. On the other hand, these material groups have poor electrical conductivity, normally. Therefore, some nano-scaled additives such as carbon black, graphene, carbon fiber, and carbon nanotube (CNT) can be used to increase the conductivity of the composites [15]. Hence, BPs can be fabricated with nanoparticle-modified fiber-reinforced polymer composites that can present lightweight structures with high electrical conductivity. Among the filler materials, CNT particles come forward owing to their superconductor structure. The addition of multi-walled CNTs increases the electrical conductivity of the thermoset resin more than the addition of single-walled CNTs [16]. The method of functionalization, employed functional groups and dimensional features of the CNTs used as additive affect also electrical conductivity of the polymers [17,18]. Moisala et al. [16] reported that the CNT particles increase the electrical conductivity of the thermoset polymers while decreasing the thermal conductivity. Through the thickness electrical conductivity of both glass fiber-reinforced and carbon fiber-reinforced polymer (CFRP) composites can be doubled with the addition of the CNTs [19]. Theoretical calculations present that the addition of the CNTs into the matrix of the FRP composites has a significant effect on the electrical properties and a limited effect on the mechanical properties of the material [20]. The detailed literature survey related to CNT-modified composite BP is presented in Table 1 [21–47]. The composition and ratios of the components investigated in composite plates, manufacturing methods, test standards and conditions, and major observations are tabulated. Hence, both similar and distinctive sides of the previous investigations are gathered under the same table. In this regard, the methods and standards on the electrical conductivities, the flexural behavior, and the fuel cell performance tests of the investigated composite bipolar plates are presented separately. Other conducted tests are given under the applied tests section. By considering the presented references, it was seen that the most preferred matrix material is polypropylene (PP) [36,37,39,42,43,46]. On the other hand, various filler materials such as expanded graphite [21,41], graphite [22–28,32–34,37,38,41–45,47], carbon black (CB) [25,35,37,40,42], carbon fiber (CF) [25,36,40,43,44,46], carbon-felt [39], graphene [43,45], metallic meshes [28] were evaluated as a second additive with MWCNT to improve the mechanical and electrical properties. It was understood that the graphite and MWCNTs filled polymers are the most common BPs in many studies. In addition, the graphene-MWCNT couple has attracted as a filler in recent years [43,45].

The Department of Energy (DOE) publishes the requirements for the bipolar plates, periodically. It is a well-known situation by the researchers, and they conduct their studies considering these necessaries. For instance, the electrical conductivity, flexural strength, and thermal conductivity properties of the bipolar plates should be > 100 S/cm, >25 MPa, and >10 W/mK, respectively [48,49]. Correlatively, MWCNT particles contribute to the electrical features of the composite structure intrinsically. However, MWCNT addition increases the properties up to a certain proportion and decreases after a threshold.

Besides, high CNT content increases the plate cost, directly. Thus, doping compensation is needed to achieve cost-effective BP fabrication.

In this study, CFRP laminates were modified with the MWCNT particles to satisfy desired BP properties as different from the existing literature. The MWCNT particles were embedded into the composite laminates with 0.25, 0.5, 0.75, 1, and 1.25% in wt., proportionally. The pristine CFRP and MWCNT modified CFRP samples were analyzed according to their electrical conductivity and flexural behavior. BP couples were machined with the pristine laminate and the MWCNT modified laminates. FC performance tests were conducted with the machined BPs and an aluminum BP. The performance curves were evaluated and compared to the aluminum alloy under the same conditions.

Experimental

Preparation of the composite plates

The CFRP laminated composite plates were manufactured with the 300 gr/cm^2 unidirectional carbon fiber fabric and epoxy system. Hexion bisphenol A type MGS L160 lamination epoxy and H160 epoxy hardener were used as an epoxy

Table 1 – Detailed literature survey related to directly CNT-modified composite BP (sorted by published date).

REF	Composition of the Investigated Composite Plate	Manufacturing Approach and Applied Tests	Mechanical Test Conditions	Electrical Conductivity Conditions	Fuel Cell Performance Test Conditions	Major Observations
[21]	Measurement of corrosion resistance 50% expanded graphite 0, 1, 2, 3, 4, 5, 6, 7, 8% CNT	Approach: Compression molding (hot press): at 50 kg/cm^2 pressure, and 80 °C for 5 min Tests: Corrosion test, density, TGA, DSC				The conductivity of the graphite/epoxy composite plate increased with the CNT modification.
[22]	Different applications on the MWCNT (MA-POA400, MA-POA 2000) 70–80% graphite 0.25, 0.5, 1, 2% MWCNT 20–30% vinyl ester	Approach: Compression molding (hot press): 140 °C for 5 min Tests: TEM, XPS, flexural strength, Raman shift, TGA.	Tests were performed according to the D790 standards. The specimen dimensions: 60 × 13 × 3 mm^3	In-plane conductivity was measured with four-point probe method. Another approach was followed for the through-plane measurements. The specimen dimensions: 30 × 30 × 3 mm^3	BP thickness is 1.2 mm. Single-cell tests were performed at 70 °C and 1 atm pressure. H_2 and air gases were supplied with 1 l/min flow rates. Active area: 4 mm^2.	The best outcomes obtained with MA-POA applied for 1% MWCNT reinforced composite plates. In addition, the FC performance of the same plate is the best after the graphite plate.
[23]	70–80% graphite 20–30% PP 0, 2, 4, 6, 8% MWCNT	Approach: Compression molding (hot press): at 70 kg/cm^2 pressure, and 170 °C for 15 min Tests: CTE measurement (ASTM D696), SEM	Tests were performed according to the D790 standards. The specimen dimensions: 60 × 13 × 3 mm^3 Unnotched Izod impact tests were performed according to the D256 standards. The Izod specimen dimensions: 64 × 13 x 12.7 × 3.3 mm^3	Electrical resistance was measured with four-point probe method.	BP thickness is 1.2 mm. Single-cell tests were performed at 60 °C and 1 atm pressure. H_2 and air gases were supplied with 1 l/min flow rates. Active area: 4 mm^2.	MWCNT addition increased the flexural strength, Izod impact, and electrical conductivity (until 4% modify). Close results were obtained in the performance tests compared to the graphite plate.
[24]	85% graphite 15% PF resin 3% CNT	Approach: Compression molding (hot press): 240 °C for 60 min Tests: TEM, FTIR, flexural strength	The specimen dimensions: 5 × 5 × 20 mm^3	The specimen dimensions: 5 × 5 × 20 mm^3		Fenton process (a kind of oxidation application) was applied to the CNT. Bending strength and conductivity increased with this application.
[25]	60–85% graphite/epoxy composite Different filler materials were added to the composite above 2.5, 5, 7.5, 10% CB 0.5, 1, 2, 3% MWCNT 1, 3, 5, 7, 9% CF Note: Values were evaluated by volume rather than by weight.	Approach: Compression molding (hot press): at 200 kg/cm^2 pressure, and 190 °C Tests: bulk density, flexural strength	Tests were performed according to the D790 standards. The specimen dimensions: 127 × 12.7 × 3.2 mm^3 Support span is 43.2 mm	In-plane conductivity was measured with four-point probe method. The specimen dimensions: 127 × 12.7 × 3.2 mm^3		Conductivity equation was provided. MWCNT was ensured the best conductivity and flexural strength magnitudes among the filler materials. A lot of figures were plotted with the variations.

[26]	65% natural graphite 35% polymeric resin 0.5, 1, 1.5, 2% MWCNT	Approach: Compression molding (hot press): at 100 kg/cm^2 pressure, and 150 °C Tests: Shore hardness, thermal conductivity, SEM, bulk density, flexural strength	Tests were performed according to the D790 standards. The specimen dimensions: 60 × 10 × 5 mm^3	In-plane and through-plane conductivities were measured with four-point probe method.	BP dimensions: 60 × 20 × 0.4 mm^3. Single-cell tests were performed at 70 °C and 83%RH. H_2 and air gases were supplied with 1.5 and 1 l/min flow rates. Nafion-1135 membrane	Conductivity increased until 1% MWCNT modify, and it has an insignificant effect above this addition. In-plane conductivity was found higher than through-plane. Also, bending strength increased by 25%.
[27]	70–80% graphite 0.25, 0.5, 1, 2% MWCNT 20–30% vinyl ester	Approach: Compression molding (hot press): at 2100 psi pressure, and 150 °C for 5 min Tests: Optical microscope				The effects of graphite – MWCNT combinations (also particle size) on the flowability characteristics of the fabricated plates were investigated.
[28]	Hybrid BP fabrication with aluminum and copper meshes 70% graphite 0–2% MWCNT 30% mesh (aluminum or copper)	Approach: Compression molding (hot press): 140 °C for 90 min Tests: FTIR, TGA, XPS, GPC, TEM, SEM		In-plane conductivity was measured with four-point probe method. Another approach (hot disk technique) was followed for the through-plane measurements. The specimen dimensions: 30 × 30 × 3 mm^3	BP thickness is 1.35 mm. Single-cell tests were performed at 70 °C and 1 atm pressure. H_2 and air gases were supplied with 1 l/min flow rates. Active area: 4 mm^2.	Through-plane conductivity and resistance measurement formulas were demonstrated. Copper mesh performed better performance compared to aluminum mesh in terms of electrical conductivity, bulk thermal conductivity, and FC performance.
[29]	MWCNT-POAMA/vinyl ester composite BP (POAMA: poly (oxyalkylene)amines bearing maleic anhydride)	Approach: Compression molding (hot press): 140 °C for 90 min Tests: FTIR, TGA, XPS, GPC, TEM, SEM, flexural strength	Tests were performed according to the D790 standards. The specimen dimensions: 60 × 13 × 3 mm^3	In-plane conductivity was measured with four-point probe method.	BP dimensions: 30 × 30 × 3 mm^3. Serpentine channel geometry with 1 mm width and depth. Active area: 4 mm^2.	Applied process increased conductivity, flexural strength, unnotched impact strength, and performance of the MWCNT.
[30]	MWCNTs/POA400-DGEBA, MWCNTs/POA2000-DGEBA, and MWCNT/PP composite BPs	Approach: Compression molding (hot press): at 70 kg/cm^2 pressure, and 170 °C for 15 min Tests: FTIR, TGA, XPS, GPC, TEM, flexural strength	Tests were performed according to the D790 standards. The specimen dimensions: 60 × 13 × 3 mm^3	Conductivity was measured with four-point probe method.	BP dimensions: 30 × 30 × 1.2 mm^3. Serpentine channel geometry with 1 mm width and depth. Single-cell tests were performed at 60 °C and 1 atm pressure. H_2 and air gases were supplied with 1 l/min flow rates.	Applied processes increased the flexural strength and conductivity properties of the MWCNT. In addition, close performance values were obtained compared to graphite plates.
[31]	MWCNT/PP-g-MA (polyethylene grafted maleic anhydride) vs. pure MWCNT comparison.	Approach: Compression molding (hot press): at 70 kg/cm^2 pressure, and 170 °C for 15 min Tests: SEM, TEM, flexural strength, Raman spectra, XPS, TGA	Tests were performed according to the D790 standards. The specimen dimensions: 60 × 13 × 3 mm^3 Support span is 50.8 mm	30 × 30 × 3 mm^3 specimens were prepared for the contact resistance measurements.	BP thickness is 1.2 mm. Single-cell tests were performed at 60 °C and 1 atm pressure. H_2 and air gases were supplied with 1 l/min flow rates.	Higher flexural strength was achieved with MWCNT/PP-g-MA composite. On the other hand, pure MWCNT has higher conductivity than MWCNT/PP-g-MA composite. In addition, close performance values were obtained compared to graphite plates.

(*continued on next page*)

Table 1 – (*continued*)

REF	Composition of the Investigated Composite Plate	Manufacturing Approach and Applied Tests	Mechanical Test Conditions	Electrical Conductivity Conditions	Fuel Cell Performance Test Conditions	Major Observations
[32]	Two different oxidation applications with the Ultraviolet ozonolysis (UV/O_3) process 75% graphite 5% MWCNT 20% epoxy	Approach: Compression molding (hot press): at 10 MPa pressure, and 130 °C for 90 min Tests: SEM, flexural strength, Vickers hardness measurement	Tests were performed according to the D790-03 standards. The specimen dimensions: 100 × 12.7 × 2.5 mm^3 Support span is 50 mm	In-plane conductivity was measured with four-point probe method. Another approach (CTU-01 from ZBT GmbH Duisburg) was followed for the through-plane measurements.		Hardness and through-plane conductivity increased with the UV/O_3 process. In other respect, flexural strength decreased with the applied oxidation approaches.
[33]	Graphite (60–80%) Epoxy (20–40%) MWCNT (1, 2.5, 5, 7.5, 10%) Eight different compositions which are composed 80% with graphite + CNT	Approach: Compression molding (hot press): at 6.2, 8.3, 10.3, and 12.4 MPa pressure, and 80, 110, 130, 150 °C for 90 min Tests: SEM, TGA, flexural strength, density measurement (according to the ASTM D792 Archimedes method)	Tests were performed according to the D790-03 standards. The specimen dimensions: 100 × 12 × 2.5 mm^3 Support span is 50.8 mm	In-plane conductivity was measured with four-point probe method. Another approach (ZBT in Duisburg, Germany) was followed for the through-plane measurements.		Desired electrical requirements are not satisfied with the unmodified plates. On the other hand, the best conductive and flexural strength structure was achieved with 5% CNT modification. The values decreased above this level.
[34]	Comparison of Wet & Dry dispersion methods 80% graphite 20% phenolic resin 0.5, 1, 1.5, 2% MWCNT	Approach: Compression molding (hot press): at 1500 psi, and 150 °C Tests: FE-SEM, TEM, flexural strength, density measurement	Tests were performed according to the ASTM D790-07 standards. Tensile tests were performed according to the ASTM D638 standards.	Four-point probe method		The schematics of the wet & dry dispersion methods were explained. The highest conductivity and flexural strength values were obtained with 1% MWCNT modified in the dry method. The magnitudes decreased above this value (1.5 and 2% MWCNT).
[35]	Textile reinforced polymer composite. Four different reinforcements were applied for the carbon fabric reinforced plastic (CFRP) material. CB and MWCNT were used to increase electrical properties. No information on the ratio of MWCNT.	Approach: Vacuum-assisted resin transfer molding (VARTM): -0.09 MPa vacuum. Tests: TEM, TGA, SEM, and viscosity measurement according to the CNT ratios.	Tests were performed according to the EN ISO 14125:1998 standards. The specimen dimensions: 80 × 10 mm^2 Support span is 60 mm	In-plane conductivity was measured with four-point probe method. Conductivity measurement formula was provided.		The schematic of the used vacuum tank was provided. Well flexural strengths were achieved. Electrical properties not increased as the level of flexural strength.

[36]	CF/PP/PE/MWCNT composite 3, 5% MWCNT Sol-gel process	Approach: Compression molding (hot press): at 20 MPa, and 220 °C for 20 min Tests: TEM, TGA, SEM, Viscosity measurement according to CNT ratio	Tests were performed according to the ASTM D790-07 standards.	In-plane conductivity was measured with four-point probe method. The specimen dimensions: $20 \times 20 \times 0.25$ mm^3 1.38 MPa pressure for the measurements.	The conductivity measurement method was given. The best results were obtained with the 5% CNT modification.
[37]	25% CB 20% PP 45–54% graphite 1–10% MWCNT 10 different BPs by changing the ratios	Approach: Compression molding (hot press): at 85 kg/cm^2 pressure, and 185 °C for 15 min Tests: Shore hardness, bulk density measurements (ASTM D792), flexural test	Tests were performed according to the ASTM D792 standards.	Conductivity was measured with four-point probe (Jandel) method.	158.32 S/cm conductivity and 30 MPa strength were obtained with 6% and 5% CNT modified composite plates, respectively. The values decreased above these ratios.
[38]	80% graphite 20% phenolic resin 0.5, 1, 1.5, 2% U-MWCNT and O-MWCNT, Si-MWCNT (unmodified and oxidized MWCNT)	Approach: Compression molding (hot press): No fabrication detail Tests: FTIR spectra, SEM, flexural strength, tensile test			Conductivity, tensile strength, and flexural strength increased with the 1% U-MWCNT and O-MWCNT modified plates. Higher flexural strength but lower conductivity was obtained with Si-MWCNT plates. Whole values decreased above 1% addition. The results were presented with tables and figures.
[39]	Carbon-felt-reinforced PP/PE/MWCNT composite 3, 5, 7% MWCNT	Approach: Compression molding (hot press): at 5 MPa pressure, and 220 °C for 20 min Tests: SEM, TGA, TEM, flexural strength	Tests were performed according to the ASTM D790-10 standards. The specimen dimensions: $50.8 \times 12.7 \times 0.4$ mm^3	A scheme was supplied to the ASR through-thickness measurements. The specimen dimensions: $100 \times 100 \times 0.4$ mm^3 0–2 MPa pressure range for the measurements.	Conductivity measurement formula was provided. CNT modification decreased the flexural strength above 3% addition of CNT. ASR measurements were given in a figure for all case studies.
[40]	MWCNT/CF/CP vs. CB/CF/EP Milled CF was used 80% CF/CP 20% EP 2, 4, 6, 8% MWCNT	Approach: Compression molding (hot press): at 1000 psi pressure, and 150 °C for 120 min Tests: SEM, flexural strength	Tests were performed according to the ASTM D638 standards.	In-plane conductivity was measured with four-point probe method (Jandel). Another approach was followed for the through-plane measurements. General effective media (GEM) approach was used for conductivity measurements.	Firstly, conductivity and flexural strength of the milled CF were investigated. Mechanical properties were found adequate, but CNT and CF additions were evaluated since the plates have poor conductivity. Hence, CNT provided a better conductive structure than CF-modified BP.

(*continued on next page*)

Table 1 – (*continued*)

REF	Composition of the Investigated Composite Plate	Manufacturing Approach and Applied Tests	Mechanical Test Conditions	Electrical Conductivity Conditions	Fuel Cell Performance Test Conditions	Major Observations
[41]	80% graphite 20% phenolic resin 0.5, 1, 1.5, 2% MWCNT Indeed, compared property is graphite variety. Synthetic graphite (SG), natural graphite (NG), expanded graphite (EG) with 80% and 20% novolac resin were used.	Approach: Compression molding (hot press): at 1800 psi pressure, and 150 °C for 90 min Tests: SEM, flexural strength, bulk density measurements (Archimedes method)	Tests were performed according to the ASTM D790 standards. The specimen dimensions: 50.8 × 12.7 × 0.9 mm^3	In-plane conductivity was measured with four-point probe method. Through-plane measurements were performed by the following of U.S. Fuel Cell Council.		CNT addition affected the flexural strength smoothly. Besides, conductivity did not increase significantly.
[42]	20% PP 25% CB 50% graphite (47–52% ratios) 5% MWCNT (3–8% ratios) 6 different compositions by varying the CNT ratio between 3 and 8%	Approach: Compression molding (hot press): at 85 kg/cm^2 pressure, and 185 °C for 20 min Tests: SEM, Shore hardness (ASTM C886), dry bulk density measurements (ASTM C559), flexural strength	Tests were performed according to the ASTM D790 standards. The specimen dimensions: 140 × 13 × 3 mm^3	In-plane conductivity was measured with four-point probe method (Jandel). Measurements were carried out at 1 mA constant current.		Results were presented with simple figures. Conductivity increased until 6% CNT reinforcement. Similarly, flexural strength was increased until a point and then decreased.
[43]	25% PP 70% milled-carbon fibre 5% MWCNT - 5% graphene 4 different compounds were formed, and CNT – graphene comparison was made.	Approach: Compression molding (hot press): at 13.8 MPa pressure, and 200 °C for 15 min Tests: SEM, XRD, Shore hardness (ASTM D2240), bulk density measurements (Archimedes method, ASTM D792), flexural strength	Tests were performed according to the ASTM D7264 standards.	In-plane conductivity was measured with four-point probe method (Jandel). Another approach was followed for the through-plane measurements.		CNT reinforcement (14.8 S/cm) provided higher conductivity (through-plane) than graphene (4.9 S/cm). Graphene (172.5 MPa) was found more strength than CNT (99.6 MPa) modify. All findings were presented in a table.
[44]	37–100% PC (polycarbonate) matrix 0–10% carbon fiber 0-10-50% graphite 3–5% CNT 7 different compounds were formed	Approach: Compression molding (hot press): at 4600 –7000 psi pressure, and 250 –300 °C for 1.5 min Tests: SEM, thermal conductivity		In-plane conductivity was measured with four probe method according to ASTM D4496. US Fuel Cell Council was followed for the through-plane measurements.		CNT, CF, graphite, and their hybrids were embedded into polycarbonate matrix. 12.8 S/cm through-plane, 8.3 S/cm in-plane, and 1.7 W/mK thermal conductivity were measured with CN3F15G45 sample.

[45]	PBA (polybenzoxazine) matrix graphite + MWCNT = 76.5% 7.5% graphene MWCNT 0–2%	Approach: Compression molding (hot press): at 150 MPa pressure, and 200 °C for 3 h Tests: Density measurements (water displacement method, ASTM D792), DSC, thermal diffusivity, water absorption (ASTM D570), SEM, TEM	Tests were performed according to the ASTM D790M standards. The specimen dimensions: 50 × 25 × 2.5 mm^3 Support span is 32 mm Crosshead speed is 0.85 mm/min	Conductivity was measured with four-point probe technique (2 × 2 cm^2 sample, Lucas Labs S-302 with SP4 head)	364 S/cm electrical conductivity, 41.5 MPa flexural strength, 49.7 GPa flexural modulus, and 21.3 W/mK thermal conductivity were measured with a 2% MWCNT modified sample.
[46]	78.5–95% PP matrix 0–20% CNF (carbon nanofiber) 0, 5, 10, 15, 20, 21.5% MWCNT 8 different compounds were formed	Approach: Compression molding (hot press): at 200 °C Tests: Microhardness (ASTM E2546), tensile tests (ASTM D638), corrosion resistance tests	Tests were performed according to the ASTM D790M standards. The specimen dimensions: 50 × 12.7 mm^2 and 1.6 –1.9 mm in thickness Support span is 25.4–27.2 – 29.6 mm (depend on thickness) Crosshead speed is 0.8 mm/min		20% MWCNT addition increased the mechanical properties. The hybrid filler of MWCNT and CNF decreased the electrochemical stability according to corrosion resistance tests.
[47]	40–65% PVDF (polyvinylidene fluoride) 33–60% graphite 0, 1, 3, 5, 7% MWCNT 10 different compounds were formed	Approach: Compression molding (hot press): at 10 MPa pressure, and 190 °C for 10 min Tests: SEM, EDS, ASR measurements, hydrophobicity tests, corrosion resistance tests	Tests were performed according to the GB/T 9341-2008 standards. Crosshead speed is 1 mm/min	In-plane conductivity was measured with four-point probe method. ASR measurements were performed to characterized through-plane conductivity.	The composite BP (5% MWCNTs and 35% graphite) exhibited electrical conductivity of 161.57 S/cm, area-specific resistances of 7.5 mΩ $cm^{2,}$ and 42.65 MPa flexural strength.

Table 2 – Specifications of MWCNT particles.

Technical Specification	Unit	Value
Outer Diameter	*nm*	10–20
Inner Diameter	*nm*	5–10
Length	*μm*	10–30
Purity	%	> 95
Specific Surface Area	m^2/g	> 200
Reel Density	g/cm^3	~ 2,1
Bulk Density	g/cm^3	0,22

system. Epoxy and epoxy hardener were mixed 100:30 by volume and resin was obtained. Specifications of the MWCNT material used in the study were presented in Table 2.

Composite plates were produced by the hot pressing technique. Composite plate manufacturing steps were illustrated in Fig. 1. In this approach, firstly CNT material was added to resin 0.25, 0.5, 0.75, 1, and 1.25% by weight, and the suspension was obtained. Then, the suspension was blended in a magnetic mixer and homogenized with an ultrasonic homogenizer. The carbon fabric layers were wetted with the homogenized epoxy/CNT suspension. Carbon fiber/epoxy laminates were stacked by hand lay-up with a sequence of $[0_4]$ and cured with a hot press under 6 bar pressure at 100 °C for 2 h. The final thickness of the laminate was ~1 mm. A water jet cutting machine was used to obtain test specimens. At this point, it was noted that the composite fabrication was limited to 1.25% by wt. CNT due to the observation of the over-cluster and agglomeration behavior of the CNT material during the mixing operation [22,46].

SEM (Scanning electron microscope) and FTIR (Fourier transform infrared spectroscopy) analyses were performed to characterize the CNT-modified samples. SEM analysis was conducted (Quanta 650 field emission SEM device) to observe CNT dispersion in the carbon fiber/epoxy laminates and the chemical reactions were detected by the FTIR (Jasco FT/IR-6700 device, in the range of 400–4000 cm^{-1}) analysis.

Electrical conductivity measurements

Electrical conductivity values were obtained using resistivity measurements of the specimens. Firstly, the specimens were produced as aforementioned in Fig. 1 and cut into 20 × 30 mm^2 dimensions. The resistances of specimens were measured by the four-point probe method (Jandel CYL-RM3000 Four Point Probe System). Then, in-plane conductivity was calculated using the sample thickness and the resistance values. The application technique of the in-plane electrical conductivity measurement is the same as the provided Refs. [44,47,50] Conductivity measurement system and equation details were given elsewhere [51].

Three-point bending flexural tests

The flexural characteristics of the pristine and MWCNT modified composites were determined according to the ASTM D790 standard. Following the instructions of the standard, the specimens were prepared in dimensions of 50.8 × 12.7 mm [39,41,46]. The specimens were then located and aligned on three point bending fixture with a 25.4 mm support span as seen in Fig. 2. The tests were performed with BESMAK BMT-10 E electro-mechanic universal test machine. The rate of crosshead motion of the machine was calculated as 1.075 mm/min with Eq. (1). The specimens were loaded until the break or the maximum strain in the outer surface reached 0.05 mm/mm. Flexural strength and flexural modulus were determined with Eqs. (2) and (3).

$$R = \frac{ZL^2}{6t} \tag{1}$$

R: *rate of crosshead motion, mm/min.*
L: *support span, mm*
t: *specimen thickness, mm.*
Z: *outer fiber's strain rate, mm/mm (Z is given as 0.01)*

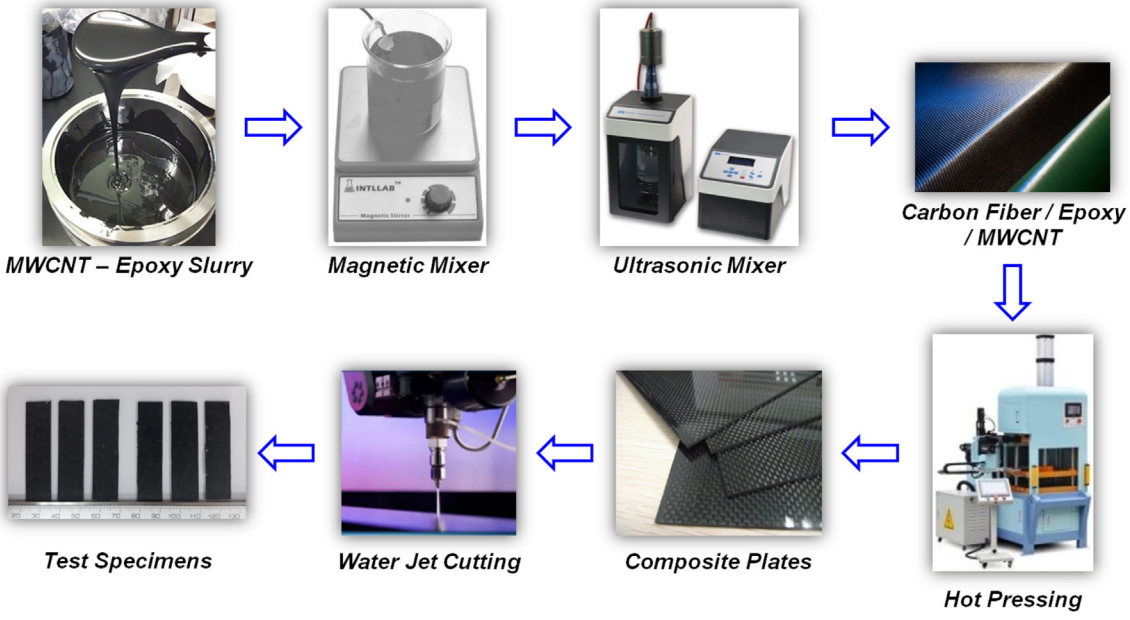


Fig. 1 – Composite plate production steps.

$$\sigma_f = \frac{3PL}{2wt^2} \quad (2)$$

$$E_f = \frac{L^3 m}{4wt^3} \quad (3)$$

Single-cell performance tests

CNT-modified bipolar plates (BPs) were fabricated for the performance measurements. Although the fabrication process was the same, BPs have a stacking sequence of $[0/90]_{10}$ and a final thickness of ~5 mm. The CNT-modified CF/epoxy composite plates were machined using the traditional machining process. The CNC-controlled milling machine was used for the machining operation. The serpentine flow channels with 1 mm in width and depth were machined on the composite plate surfaces. Then, gas inlet and outlet holes were processed, and each CNT modified (0.25, 0.5, 0.75, 1, and 1.25% in wt.) composite BP couple was obtained. Commercially available 5-layer air-MEAs (membrane electrode assembly) having 25 cm^2 active area were purchased and used in the single-cell tests [52]. In consequence, BPs were manufactured with a 25 cm^2 active area and 80 × 80 × 5 cm^3 total dimensions depending on the active area of the MEA. Fabricated CNT modified composite BPs and other components of the short stack were illustrated in Fig. 3. The gold-coated stainless steel current collectors and the stainless steel 316l end plates were used to inhibit performance losses due to the contact resistance. An environmental chamber was used to achieve operating temperature and the tests were performed at 50 °C. 0.4 and 1.2 lt/min H_2 and air gases were supplied to the anode and cathode compartments, respectively. The standard Electrochem, Inc. Fuel Cell Test Station was used to supplying of the gases, loading, and current data collection. The MEA was activated before the tests according to the applied activation process in Ref. [53] In addition, the performance results of the CNT modified composite BPs were compared to AA 3105 aluminum alloy under the same operating conditions. The reason for the AA 3105 selection is the high fuel cell test performance of AA 3105 and the high corrosion resistance of the 3000-series aluminum alloys [54]. The performance tests were conducted as short-term for 2 h. The polarization curves were recorded after stability was ensured in the current and voltage values.

Results and discussion

Physico-chemical characterization

SEM images of the pristine CFRP and CNT-modified CFRP specimens were presented in Fig. 4. The images at each row have a magnification of 5.000, 20.000, and 50.000 respectively. A smooth surface of fiber was seen in the micrographs of the pristine specimens. On the other hand, CNTs were located on the fibers with some amount of epoxy. We have observed that CNTs supplied better bonding between epoxy and carbon fibers than that of the pristine specimens. SEM images proved that the CNTs were well dispersed in the resin (see Fig. 5).

FTIR examination proved the interface bonding between CNT and epoxy as understood in Fig. 6. The chemical bonds and the existence of the functional groups were presented. The peaks of the pristine CFRP/epoxy structure fully matched the literature. Kumar et al. [55] reported the peaks at 824, 1243, and 2919 cm^{-1} confirmed the existence of epoxy functional groups in the carbon fiber structure. The same peaks were

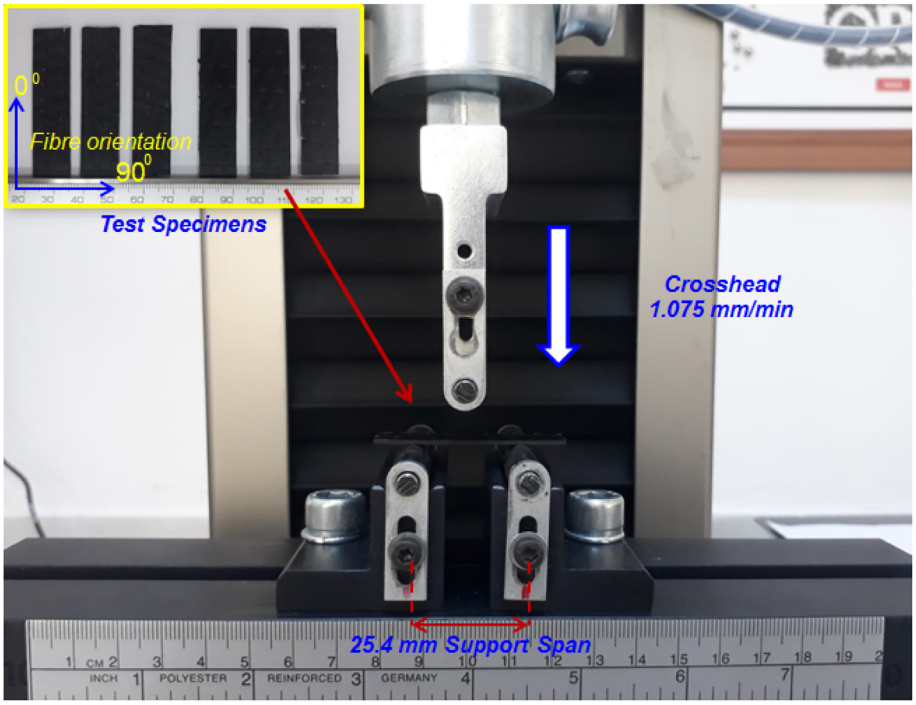


Fig. 2 – Three-point bending flexural test bench.

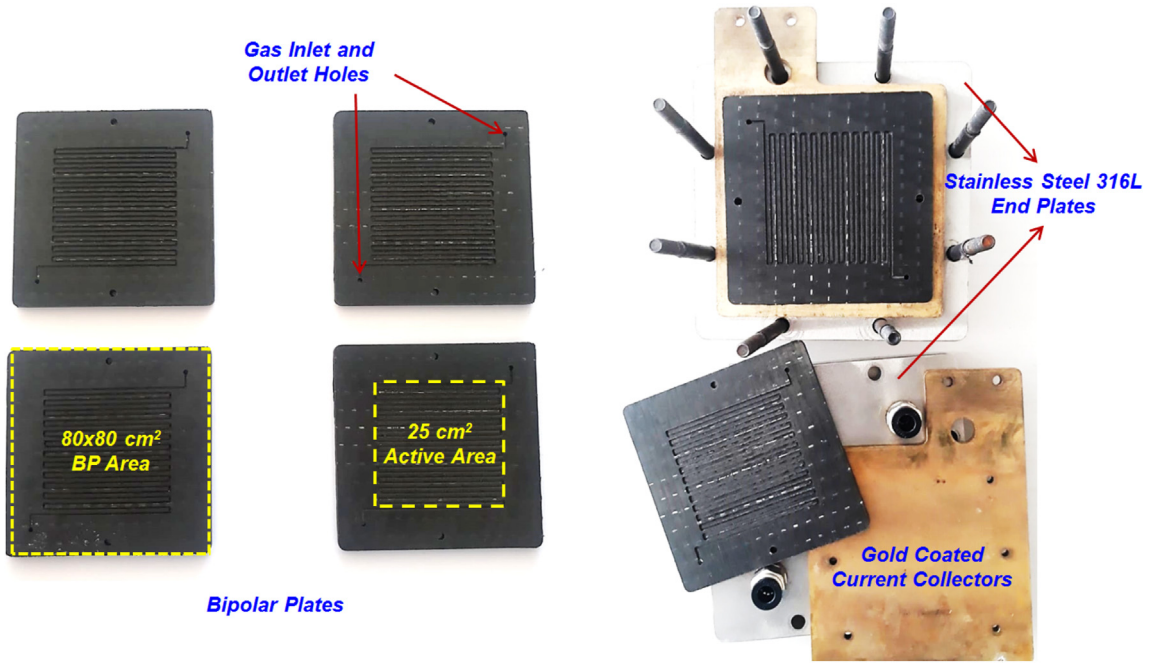


Fig. 3 – MWCNT modified composite BPs and single-cell stack configuration.

observed respectively at 826, 1235, and 2920 cm^{-1} in the current study as presented in Fig. 6. C–O bond stretching was observed at 1028, 1180, and 1454 cm^{-1}. The same stretching peaks were observed at 1042 [58,62], 1048 [61], 1165 [60], 1182 [57], 1420 [58] cm^{-1}. C=C symmetric stretching was detected at 1606 cm^{-1} as reported at 1625 [58], 1630 [57,59], 1634 [60] cm^{-1}, in the literature.

Carbonyl group (C=O bonds) was noted at 1704 [57], 1716 [60], 1731 [62], 1760 [56], 1795 [61] cm^{-1} and it was recorded at 1731 cm^{-1} in this study. C–H stretching was observed between 2917 and 2922 cm^{-1}. Similar bonds were stated at 2680 [59], 2885 [59], 2920 [58], 2925 [62]. Finally, the hydroxyl groups (O–H stretching) were observed in the range of 3291–3348 cm^{-1} as reported at 3400 [55], 3430 [58], 3432 [55], 3438 [57], 3440 [60], 3468 [62], 3550 [56,61] cm^{-1}. It is reported that gliding occurred in the bands with the CNT modification to the epoxy resin [55]. And also this approved the good interaction between structures.

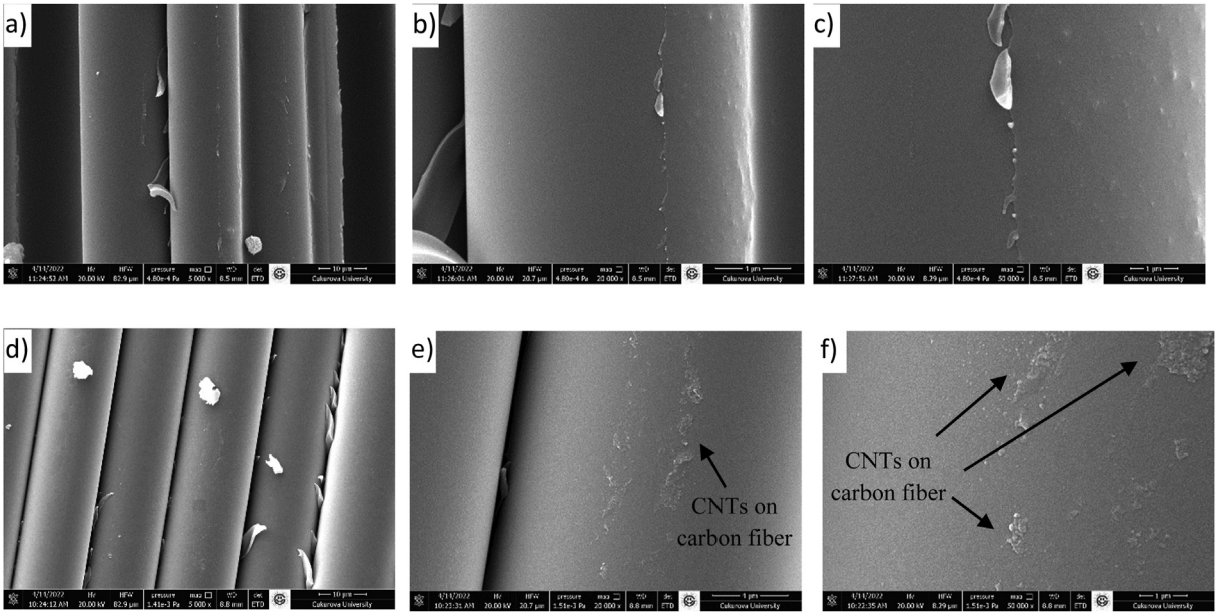


Fig. 4 – SEM images of the pristine CFRP (a–c) and CNT modified CFRP specimens (d–f).

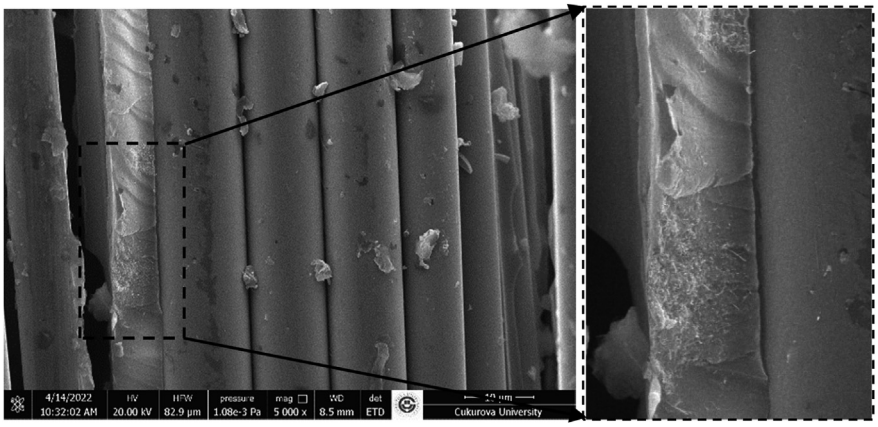


Fig. 5 – Distribution of the CNTs in epoxy resin.

Electrical conductivity

We measured the in-plane electrical conductivity of the BPs rather than through-plane measurements. In-plane conductivity values of the composite structures were found higher than through-plane conductivities in many studies in the existing literature. Liao et al. [22] determined the in-plane and through-plane electrical conductivities of the 1% pristine-MWCNT modified nanocomposite BPs as 513 and 27.9 S/cm, respectively. Dhakate et al. [26] reported that the in-plane and through-plane conductivities of the graphite-polymer-based composite BPs increased with the MWCNT reinforcement until a 1% ratio, and reached 178 and 30 S/cm, respectively. Similarly, 513 S/cm in-plane conductivity was achieved with 1% MWCNT-POAMA BP while 37.8 S/cm through-plane was calculated by Hsiao et al. [28] Similar trends were observed in Refs. [32,33] Therefore, through-plane measurements were not conducted, and in-plane conductivity calculations were pointed out as adequate and appropriate in terms of DOE targets.

In-plane electrical conductivity pre-test results of the 0.25, 0.5, 0.75, and 1% CNT modified composite plates were calculated in the previous paper study by the authors [51]. The highest electrical conductivity 94.58 S/cm was achieved with a 1% CNT plate. Although this highest value is pretty close to DOE requirements (>100 S/cm), it is still under the target. Therefore, the CNT ratio was increased proportionally, and a 1.25% CNT modified plate was prepared in this study to satisfy electrical expectations. Finally, 120.05 S/cm conductivity was measured for a 1.25% CNT modified plate. Whole conductivity values were presented in Fig. 7. 49.35, 56.28, 64.3, 94.58, and 120.05 S/cm conductivity values were measured for the 0.25, 0.5, 0.75, 1, and 1.25% CNT modified composite plates, respectively. It was seen that the CNTs can supply the desired conductivity for CF/epoxy composite BPs. In this context, a 1.25% CNT modified BP was appropriate in terms of the DOE targets.

The electrical conductivity values increase continuously as seen in Fig. 7. The authors tried to determine a threshold that explains the conductivity-CNT ratio relationship. The

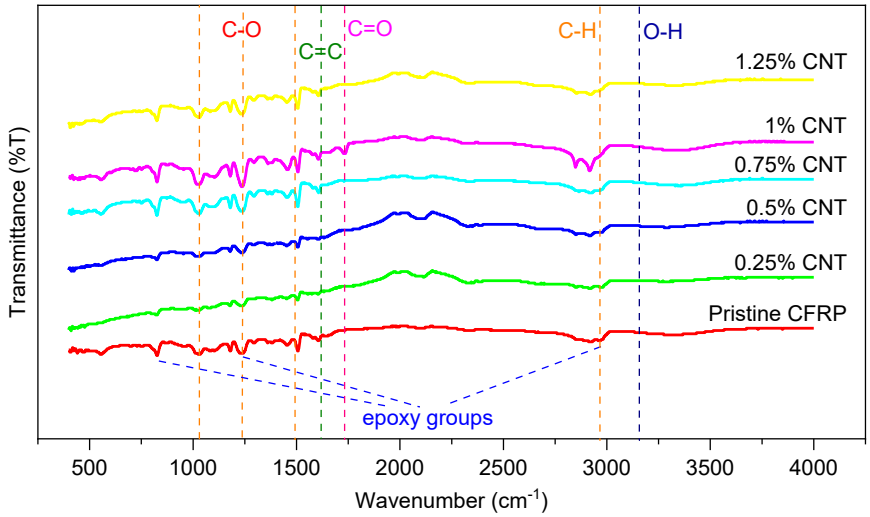


Fig. 6 – FTIR spectra of the pristine CFRP and MWCNT modified CFRP specimens.

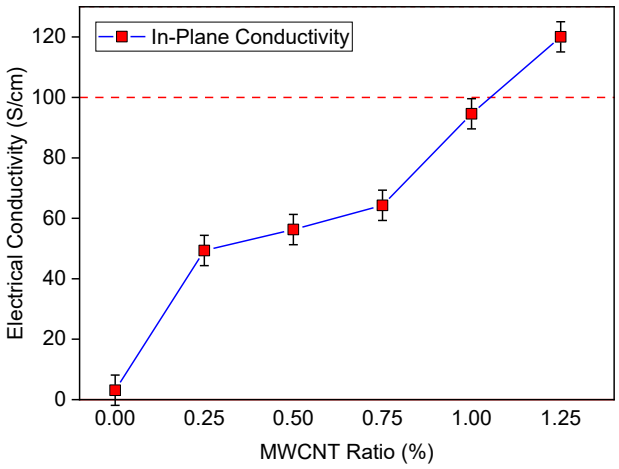


Fig. 7 – Electrical conductivity values of the CNT modified composite plates.

specimen manufacturing failed above 1.25% CNT modification due to the CNT cluster mechanism breaking the conductivity chains between particles. It is thought that the conductivity will be decreased above 1.25% CNT modification because of the agglomeration behavior of the CNT particles. Nonetheless, a threshold for the electrical conductivity could not be determined due to the specimen manufacturing failure above the aforementioned CNT modification.

However, high CNT modification may not contribute to the electrical conductivity properties all the while. It was noted in many studies that the CNT modification decreased the conductivity above 1% [22,26,28,29,34,38]. Liao and co-workers [23] stated that the CNT doping increased the conductivity until 4% reinforcement. Above this modification (until 8%), it decreased electrical properties. Suherman et al. [33] and Hu et al. [47] reported that the CNTs with a weight ratio higher than 5% do not improve the electrical conductivity. Similarly, a rise in the electrical conductivity of the CNTs modified composites can be provided until a modification ratio of 6%, and then the conductivity decreases with more CNTs [37,40,42]. In this regard, optimization of the CNT modification ratio is crucial in terms of reducing the BP fabrication costs due to the high price of the CNT. Otherwise, it causes negative effects on cost accounting easily [63]. Besides, the primary reason for the electrical conductivity decrease with the usage of CNTs higher than a threshold ratio is the cluster behavior of the CNT in the polymer matrix. The cluster of CNTs causes an increase in the distance of CNT agglomerations and relatively inhibits the CNT molecule connections horizontally and vertically [22,46,63].

Flexural strength tests

Flexural strength and flexural modulus findings of the composite reinforced with 0° and 90° fibers are illustrated in Figs. 8 and 9, respectively.

The addition of the MWCNTs has obvious improvement on the flexural properties of the carbon/epoxy laminated composites. The flexural strength of the composite reinforced with 0° fibers (longitudinal flexural strength) increased from 0.99 GPa up to 1.41 GPa with a weight ratio of 1.25% of MWCNTs. This means an increment of 42% when compared with the pristine composite. Similarly, the flexural strength of the composite reinforced with 90° fibers (transverse flexural strength) increased up to 47.43 GPa with a weight ratio of 0.75% of MWCNTs. And this corresponds to an increment of 39.83% according to the pristine composite. The weight fraction of 0.75% is a threshold to observe the significant improvement of MWCNTs on the flexural properties of the carbon/epoxy composite.

Although not as significant as the increase in flexural strength, the flexural modulus of the composite also increased with the addition of MWCNT. The change in flexural modulus of the composite with the MWCNT additive ratio by weight has a similar trend to the change in flexural strength. The

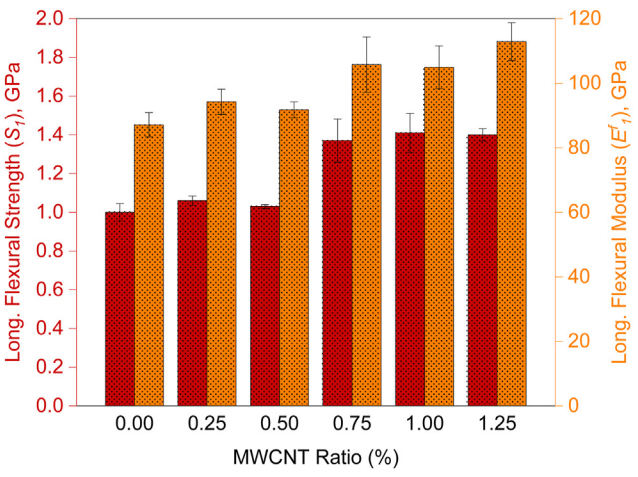


Fig. 8 – Flexural strength and flexural modulus of the composite reinforced with 0° fibers for various MWCNT ratios.

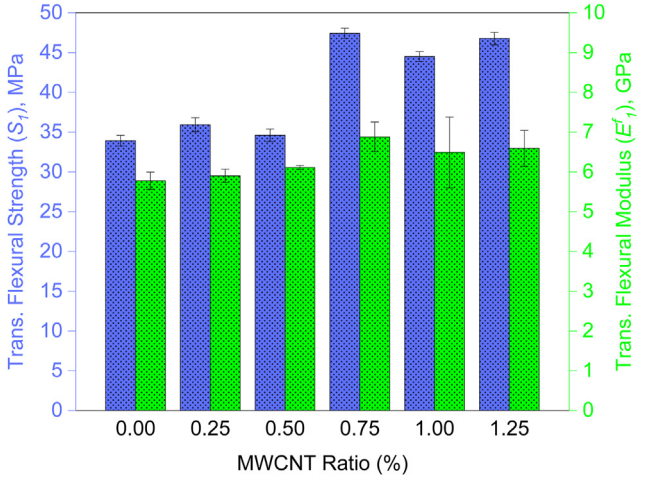


Fig. 9 – Flexural strength and flexural modulus of the composite reinforced with 90° fibers for various MWCNT ratios.

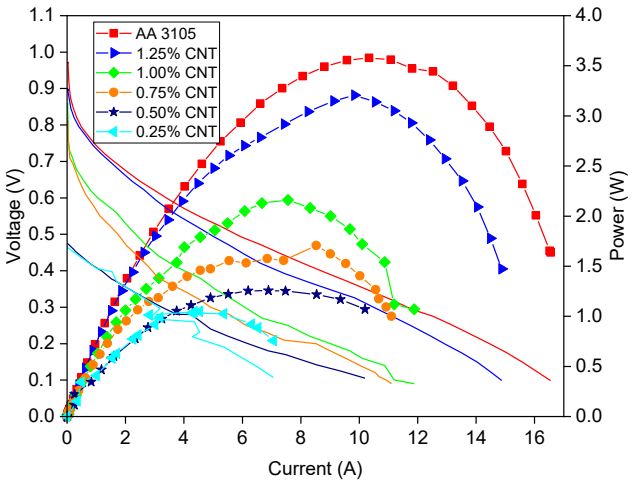


Fig. 10 – I–V curves of the MWCNT modified BPs and AA 3105 alloy BP.

weight ratio of 0.75% is the critical ratio to improve the flexural modulus of the composite. The tests proved that according to the pristine composite it is possible to increase the flexural modulus of 0° reinforced composite by 26.73% and the flexural modulus of 90° reinforced composite by 19.12%. However, Sharma and Shukla [64] reported that the flexural properties of the hand layed-up carbon/epoxy laminates could be enhanced by adding functionalized MWCNTs up to a weight ratio of 1.5%. Shen et al. [65] specified the optimum weight ratio of MWCNTs as 0.5% to improve the flexural strength and as 1% to improve the flexural modulus of the E-glass/epoxy composites.

The influence of the MWCNT modification on the mechanical properties is not as high as it affects the electrical properties. Although the MWCNT addition does not usually bring about a decrease, it negatively affects the mechanical properties after a certain rate. Namely, the existence of a threshold which is the peak MWCNT reinforcement point for the flexural properties was addressed in many studies [26,33,34,37,38,40,42]. On the other hand, MWCNT addition increased the flexural strength continuously in some investigations as in the present study [22,23,29–31,45,47]. This means that the peak flexural strength has not yet been reached. The mentioned situation is experienced in low CNT loadings, commonly. Whereas, a threshold in the flexural features is seen in high CNT modifications [33,37,40,42].

Performance tests

Polarization curves of the CNT-modified composite BPs and AA 3105 BP are presented in Fig. 10. It is seen that the net power output increased with the CNT modification. 3.21 W peak power was achieved with a 1.25% CNT modified composite plate under specified conditions, and the power value was decreased with the diminishing CNT ratio. On the other hand, 3.56 W net power was obtained with AA 3105 aluminum alloy BP. The open circuit voltage (OCV) was at the 0.97 V levels initially for the AA 3105 BP. The OCVs of the 1.25, 1, and 0.75% CNT modified BPs were 0.9, 0.85, and 0.81 levels, respectively, before the current drawn. Nevertheless, highly poor OCVs were reached with 0.5 (0.48 V) and 0.25% (0.47) CNT added BPs. Inconsistent behavior of the low-CNT filled BPs was revealed with the polarization curves, especially at the high current levels. Poor electrical properties of the low-CNT modified BPs resulted in discontinuity and low performance. In other respects, 1.25% CNT-filled composite BP has performed a pretty close power output compared to the AA 3105 alloy.

The short-term (2 h) performance tests were conducted for all cases and the H_2 and the air gases were supplied to the stack during the tests. Then, the polarization curves were recorded after stability was ensured in the current and voltage values. Fluctuant voltage and current behavior were observed with the 0.25 and 0.5% CNT-modified BP tests. It was shown when the polarization curves were taken. The cell behaved unstable, especially at peak loads. On the other hand, consistent values were recorded at high CNT modifications, especially 1 and 1.25% modified BPs. Voltage and current maintained stable position during the test and polarization curve saving step. It proved the stability of the manufactured BPs with high CNT modification. In addition, the performance test results were matched with the electrical conductivity measurements. A rising trend was observed in the performance test results with the CNT-modification increase as in the conductivity values.

It is obviously demonstrated that the fuel cell tests were performed particularly in earlier studies than the recent research (Table 1). In general, the researchers focused on the mechanical and electrical features of the nanoparticle-modified composite plates than the performance characterizations in the previous years. As an example of the earlier studies, Liao et al. [22] functionalized the MWCNT particles with MA-POA molecules, manufactured composite BPs with 1.2 mm in thickness, and evaluated the FC performance of their BPs. The applied process improved the MWCNT features and close performance was achieved compared to the graphite BP. Similar results were obtained in other studies by the same group [23,29,30]. Dhakate et al. [26] manufactured CNT (0–2%)-modified natural graphite-epoxy composite BPs with 60 × 20 × 0.4 mm^3 in dimensions and tested at 70 °C and 83% RH. 1.5H_2 and 1 lt/min air gases were supplied to the short stack and it was reported that the fabricated NPL BP performed higher power density than the commercial Schunk BP. An interesting hybrid BP fabrication was made by Hsiao et al. [28] They manufactured graphite-mesh (aluminum or copper) composites with 1.35 mm in thickness and functionalized them with MWCNT (0–2%). The same test conditions were followed by Ref. [22], and it was stated that the composite BP with copper mesh showed better performance than hybrid BP with aluminum mesh.

However, the performance comparison between the current study and the existing literature is not possible due to the material differences and operating conditions. Nonetheless, the performance tests were conducted for the MWCNT modified composite BPs and compared with AA 3105 aluminum alloy. Considering the lightweight structures of composite BPs, the investigated CNT modified CF/epoxy BP may significantly contribute to the effort on the reduction of PEMFC stack weight [66].

Conclusion

Lightweight structures are the most highlighted features of composite plates. They may be potential alternative bipolar plates when modified with superconductive nanomaterials. MWCNT group has prominent characteristics to compensate required electrical properties of the composite plates. In the present study, MWCNT particles were filled into carbon fiber-epoxy composite laminates in the range of 0–1.25% in wt. and tested in terms of electrical, mechanical, and performance characteristics. The increment of the CNT reinforcement increased the electrical properties, as expected, and 120.05 S/cm in-plane conductivity was achieved with a 1.25% CNT modified composite specimen. CNTs increased also the longitudinal and transverse flexural strengths of the CFRP by up to 40% compared with the pristine composite plates. By considering the importance of the flexural strength for BPs, the addition of CNTs into CFRP benefit the durability of the BPs. Hence, it was confirmed that the electrical and mechanical properties were at the desired level for the BP application. However, specified characteristics are being restricted due to the structural deficiencies and agglomeration behavior of the CNT particles above a threshold proportion. Clustered CNT groups lead to gaps between CNT molecules and relatively break the horizontal and vertical CNT connections locally. In this regard, optimization of the CNT modification ratio is needed to hinder excessive material utilization and achieve cost-effective BP. Finally, the fabricated CNT modified BPs were conducted to the performance tests and compared with AA 3105 aluminum alloy. 1.25% CNT-filled composite BP exhibited close performance to the aluminum plate and 3.21 and 3.56 peak power values were obtained for the composite and aluminum BPs, respectively. In this case, there is no doubt against the use of CNT modified composites as BP in the PEMFC system. Moreover, the lightweight structure of the composite BP will be contributed to the stack weight reduction endeavor.

Declaration of competing interest

The authors declare that they have no known competing financial interests or personal relationships that could have appeared to influence the work reported in this paper.

Acknowledgments

The authors acknowledge the partial support provided by the Office of Scientific Research Projects of Çukurova University under Contract No. FDK-2020-12750.

REFERENCES

[1] Darıcık F, Topcu A, Tüccar G, Aydın K. Effects of fibre orientations and flow channel patterns on the durability of composite bipolar plates used in PEMFCs. In: IEEE, 8th *international Conference on modeling, Simulation and applied optimization*; 2019. https://doi.org/10.1109/ICMSAO.2019.8880456. Bahrain.

[2] Topcu M, Topcu A, Aydın K, Çelik S, Koçak NF. Traditional and innovative manufacturing techniques of bipolar plates used in PEM fuel cell. Acad Persp Proc 2019;2(3):720–9. https://doi.org/10.33793/acperpro.02.03.79.

[3] Nandjou F, Poitor-Crouvezier J-P, Chandesris M, Rosini S, Hussey DS, Jacobson DL, LaManna JM, Morin A, Bultel Y. A pseudo-3D model to investigate heat and water transport in large area PEM fuel cells – Part 2: application on an automotive driving cycle. Int J Hydrogen Energy 2016;41:15573–84. https://doi.org/10.1016/j.ijhydene.2016.06.007.

[4] Sankar K, Jana AK. Nonlinear multivariable sliding mode control of a reversible PEM fuel cell integrated system. Energy Convers Manag 2018;171:541–65. https://doi.org/10.1016/j.enconman.2018.05.079.

[5] Paul B, Andrews J. PEM unitised reversible/regenerative hydrogen fuel cell systems: state of the art and technical challenges. Renew Sustain Energy Rev 2017;79:585–99. https://doi.org/10.1016/j.rser.2017.05.112.

[6] Rivarolo M, Rattazzi, Lamberti T, Magistri L. Clean energy production by PEM fuel cells on tourist ships: a time-dependent analysis. Int J Hydrogen Energy 2020;45(47):25747–57. https://doi.org/10.1016/j.ijhydene.2019.12.086.

[7] Gadalla M, Zafar S. Analysis of a hydrogen fuel cell-PV power system for small UAV. Int J Hydrogen Energy 2016;41:6422–32. https://doi.org/10.1016/j.ijhydene.2016.02.129.

[8] Gong A, Verstraete D. Fuel cell propulsion in small fixed-wing unmanned aerial vehicles: current status and research needs. Int J Hydrogen Energy 2017;42:21311–33. https://doi.org/10.1016/j.ijhydene.2017.06.148.

[9] Ghosh A, Goswami P, Mahanta P, Verma A. Effect of carbon fiber length and graphene on carbon-polymer composite bipolar plate for PEMFC. J Solid State Electrochem 2014;18:3427–36. https://doi.org/10.1007/s10008-014-2573-1.

[10] Song Y, Zhang C, Ling C-Y, Han M, Yong R-Y, Sun D, Chen J. Review on current research of materials, fabrication and application for bipolar plate in proton exchange membrane fuel cell. Int J Hydrogen Energy 2019;45(54):29832–47. https://doi.org/10.1016/j.ijhydene.2019.07.231.

[11] Evangelisti S, Tagliaferri C, Brett DJL, Lettieri P. Life cycle assessment of a polymer electrolyte membrane fuel cell system for passenger vehicles. J Clean Prod 2017;142:4339–55. https://doi.org/10.1016/j.jclepro.2016.11.159.

[12] Manufacturing cost analysis of PEM fuel cell systems for 5- and 10-kW backup power applications. https://www.energy.gov/sites/prod/files/2016/12/f34/fcto_cost_analysis_pem_fc_5-10kw_backup_power_0.pdf. [Accessed 2 April 2021].

[13] Karacan K, Celik S, Toros S, Alkan M, Aydin U. Investigation of formability of metallic bipolar plates via stamping for light-weight PEM fuel cells. Int J Hydrogen Energy 2020;45:35149–61. https://doi.org/10.1016/j.ijhydene.2020.01.251.

[14] Taherian R. A review of composite and metallic bipolar plates in proton exchange membrane fuel cell: materials, fabrication, and material selection. J Power Sources 2014;265:380–90. https://doi.org/10.1016/j.jpowsour.2014.04.081.

[15] Yeetsorn R, Fowler MW, Tzoganakis C. A review of thermoplastic composites for bipolar plate materials in PEM fuel cells, nanocomposites with unique properties and applications in medicine and industry. Dr John Cuppoletti

(Ed.), ISBN: 978-953-307-351-4, InTech, Available from: http://www.intechopen.com/books/nanocomposites-with-unique-properties-and-applications-in-medicineand-industry/a-review-of-thermoplastic-composites-for-bipolar-plate-materials-in-pem-fuel-cells.
[16] Moisala A, Li Q, Kinloch IA, Windle AH. Thermal and electrical conductivity of single- and multi-walled carbon nanotube-epoxy composites. Compos Sci Technol 2006;66:1285–8. https://doi.org/10.1016/j.compscitech.2005.10.016.
[17] Kim YJ, Shin TS, Choi HD, Kwon JH, Chung YC, Yoon HG. Electrical conductivity of chemically mdified multiwalled carbon nanotube/epoxy composites. Carbon 2005;43:23–30. https://doi.org/10.1016/j.carbon.2004.08.015.
[18] Sagar R, Petrova RS, Somenath M. Effect of carbon nanotube (CNT) functionalization in Epoxy-CNT composites. Nanotechnol Rev 2018;7:475–85. https://doi.org/10.1016/j.physbeh.2017.03.040.
[19] da Costa EFR, Skordos AA, Partridge IK, Rezai A. RTM processing and electrical performance of carbon nanotube modified epoxy/fibre composites. Compos Part A Appl Sci Manuf 2012;43:593–602. https://doi.org/10.1016/j.compositesa.2011.12.019.
[20] Daricik F, Topcu A. Theoretical analysis on the thermal and electrical properties of fiber reinforced laminates modified with CNTs. Çukurova Univ J Facul Eng Arch 2020;35(4):925–36.
[21] Lee HK, Rim HR, Lee JY, Lee J, Yoon JM, Bae W, Yang SW. Improvements of electrical properties containing carbon nanotube in epoxy/graphite bipolar plate for polymer electrolyte membrane fuel cells. J Nanosci Nanotechnol 2008;8:5464–6. https://doi.org/10.1166/jnn.2008.1135.
[22] Liao S-H, Yen C-Y, Hung C-H, Weng C-C, Tsai M-C, Lin Y-F, Ma C-CM, Pan C, Su A. One-step functionalization of carbon nanotubes by free-radical modification for the preparation of nanocomposite bipolar plates in polymer electrolyte membrane fuel cells. J Mater Chem 2008;18:3993–4002. https://doi.org/10.1039/b806054a.
[23] Liao S-H, Yen C-Y, Weng C-C, Lin Y-F, Ma C-CM, Yang C-H, Tsai M-C, Yen M-Y, Hsiao M-C, Lee S-J, Xie X-F, Hsiao Y-H. Preparation and properties of carbon nanotube/polypropylene nanocomposite bipolar plates for polymer electrolyte membrane fuel cells. J Power Sources 2008;185:1225–32. https://doi.org/10.1016/j.jpowsour.2008.06.097.
[24] Yin Q, Sun K-n, Li A-j, Shao L, Liu S-m, Sun C. Study on carbon nanotube reinforced phenol formaldehyde resin/graphite composite for bipolar plate. J Power Sources 2008;175:861–5. https://doi.org/10.1016/j.jpowsour.2007.10.013.
[25] Lee JH, Jang YK, Hong CE, Kim NH, Li P, Lee HK. Effect of carbon fillers on properties of polymer composite bipolar plates of fuel cells. J Power Sources 2009;193:523–9. https://doi.org/10.1016/j.jpowsour.2009.04.029.
[26] Dhakate SR, Sharma S, Chauhan N, Seth RK, Mathur RB. CNTs nanostructuring effect on the properties of graphite composite bipolar plate. Int J Hydrogen Energy 2010;35:4195–200. https://doi.org/10.1016/j.ijhydene.2010.02.072.
[27] Hsiao M-C, Liao S-H, Yen M-Y, Su A, Wu I-T, Hsiao M-H, Lee S-J, Teng C-C, Ma C-CM. Effect of graphite sizes and carbon nanotubes content on flowability of bulk-molding compound and formability of the composite bipolar plate for fuel cell. J Power Sources 2010;195:5645–50. https://doi.org/10.1016/j.jpowsour.2010.03.065.
[28] Hsiao M-C, Liao S-H, Yen M-Y, Ma C-CM, Lee S-J, Chen Y-H, Hung C-H, Lin Y-F, Xie X-F. Electrical and thermal conductivities of novel metal mesh hybrid polymer composite bipolar plates for proton exchange membrane fuel cells. J Power Sources 2010;195:509–15. https://doi.org/10.1016/j.jpowsour.2009.06.065.
[29] Liao S-H, Hsiao M-C, Yen C-Y, Ma C-CM, Lee S-J, Su A, Tsai M-C, Yen M-Y, Liu P-L. Novel functionalized carbon nanotubes as cross-links reinforced vinyl ester/nanocomposite bipolar plates for polymer electrolyte membrane fuel cells. J Power Sources 2010;195:7808–17. https://doi.org/10.1016/j.jpowsour.2009.10.020.
[30] Liao S-H, Weng C-C, Yen C-Y, Hsiao M-C, Ma C-CM, Tsai M-C, Su A, Yen M-Y, Lin Y-F, Liu P-L. Preparation and properties of functionalized multiwalled carbon nanotubes/polypropylene nanocomposite bipolar plates for polymer electrolyte membrane fuel cells. J Power Sources 2010;195:263–70. https://doi.org/10.1016/j.jpowsour.2009.06.064.
[31] Hsiao M-C, Lin Y-F, Tsai HM, Ma C-CM, Lee S-H, Yen M-Y, Liu P-I. Polypropylene-grafted multi-walled carbon nanotube reinforced polypropylene composite bipolar plates in polymer electrolyte membrane fuel cells. Energy Environ Sci 2011;4:543–50. https://doi.org/10.1039/c0ee00057d.
[32] Royan NRR, Sulong AB, Sahari J, Suherman H. Effect of acid- and ultraviolet/ozonolysis-treated MWCNTs on the electrical and mechanical properties of epoxy nanocomposites as bipolar plate applications. J Nanomater 2013:717459 1–8. https://doi.org/10.1155/2013/717459.
[33] Suherman H, Sulong AB, Sahari J. Effect of compression molding parameters on the in-plane and through-plane conductivity of carbon nanotubes/graphite/epoxy nanocomposites as bipolar plate material for a polymer electrolyte membrane fuel cell. Ceram Int 2013;39:1277–84. https://doi.org/10.1016/j.ceramint.2012.07.059.
[34] Chaiwan P, Pumchusak J. Wet vs. dry dispersion methods for multiwall carbon nanotubes in the high graphite content phenolic resin composites for use as bipolar plate application. Electrochim Acta 2015;158:1–6. https://doi.org/10.1016/j.electacta.2015.01.101.
[35] Jiang B, Stübler N, Wu W, Li Q, Ziegmann G, Meiners D. Manufacturing and characterization of bipolar fuel cell plate with textile reinforced polymer composites. Mater Des 2015;65:1011–20. https://doi.org/10.1016/j.matdes.2014.10.044.
[36] Lee HE, Han SH, Song SA, Kim SS. Novel fabrication process for carbon fiber composite bipolar plates using sol gel and the double percolation effect for PEMFC. Comp Struct 2015;134:44–51. https://doi.org/10.1016/j.compstruct.2015.08.037.
[37] Bairan A, Selamat MZ, Sahadan SN, Malingam SD, Mohamad N. Effect of carbon nanotubes loading in multifiller polymer composite as bipolar plate for PEM fuel cell. Procedia Chem 2016;19:91–7. https://doi.org/10.1016/j.proche.2016.03.120.
[38] Chaiwan P, Sarakonsri T, Pumchusak J. Electrical and mechanical properties of surface functionalized carbon nanotubes incorporated graphite-phenolic composite bipolar plate for PEMFC. Key Eng Mater 2016;707:23–7. https://doi.org/10.4028/www.scientific.net/KEM.707.23.
[39] Lee HE, Chung YS, Kim SS. Feasibility study on carbon-felt-reinforced thermoplastic composite materials for PEMFC bipolar plates. Comp Struct 2017;180:378–85. https://doi.org/10.1016/j.compstruct.2017.08.037.
[40] Radzuan NAM, Zakaria MY, Sulong AB, Sahari J. The effect of milled carbon fibre filler on electrical conductivity in highly conductive polymer composites. Composites B 2017;110:153–60. https://doi.org/10.1016/j.compositesb.2016.11.021.
[41] Yao K, Adams D, Hao A, Zheng JP, Liang Z, Nguyen N. Highly conductive and strong graphite-phenolic resin composite for

bipolar plate applications. Energy Fuels 2017;31:14320–31. https://doi.org/10.1021/acs.energyfuels.7b02678.
[42] Bairan A, Selamat MZ, Sahadan SN, Malingam S, Mohamad N. Effect of CNTs on the electrical and mechanical properties of polymeric composite as PEM fuel cell bipolar plate. J Teknol 2018;80(6):115–22. https://doi.org/10.11113/jt.v80.10774.
[43] Radzuan NAM, Sulong AB, Somalu MR, Abdullah AT, Husaini T, Rosli RE, Majlan EH, Rosli MI. Fibre orientation effect on polypropylene/milled carbon fiber composites in the presence of carbon nanotubes or graphene as a secondary filler: application on PEM fuel cell bipolar plate. Int J Hydrogen Energy 2019;44:30618–26. https://doi.org/10.1016/j.ijhydene.2019.01.063.
[44] Naji A, Krause B, Pötschke P, Ameli A. Hybrid conductive filler/polycarbonate composites with enhanced electrical and thermal conductivities for bipolar plate applications, Polym. Composer 2019;40:3189–98. https://doi.org/10.1002/pc.25169.
[45] Witpathomwong S, Okhawilai M, Jubsilp C, Karagiannidis P, Rimdusit S. Highly filled graphite/graphene/carbon nanotube in polybenzoxazine composites for bipolar plate in PEMFC. Int J Hydrogen Energy 2020;45:30898–910. https://doi.org/10.1016/j.ijhydene.2020.08.006.
[46] Ramírez-Herrera CA, Tellez-Cruz MM, Pérez-González J, Solorza-Feria O, Flores-Vela A, Cabanas-Moreno JG. Enhanced mechanical properties and corrosion behavior of polypropylene/multi-walled carbon nanotubes/carbon nanofibers nanocomposites for application in bipolar plates of proton exchange membrane fuel cells. Int J Hydrogen Energy 2021;46:26110–25. https://doi.org/10.1016/j.ijhydene.2021.04.125.
[47] Hu B, Chang F-L, Xiang L-Y, He G-J, Cao X-W, Yin X-C. High performance polyvinylidene fluoride/graphite/multi-walled carbon nanotubes composite bipolar plate for PEMFC with segregated conductive networks. Int J Hydrogen Energy 2021;46:25666–76. https://doi.org/10.1016/j.ijhydene.2021.05.081.
[48] Kakati BK, Sathiyamoorthy D, Verma A. Electrochemical and mechanical behavior of carbon composite bipolar plate for fuel cell. Int J Hydrogen Energy 2010;35:4185–94. https://doi.org/10.1016/j.ijhydene.2010.02.033.
[49] Kakati BK, Ghosh A, Verma A. Efficient composite plate reinforced with carbon fiber and graphene for proton exchange membrane fuel cell. Int J Hydrogen Energy 2013;38:9362–9. https://doi.org/10.1016/j.ijhydene.2012.11.075.
[50] Radzuan NAM, Sulong AB, Somalu MR. Influence the filler orientation on the performance of bipolar plate. Sains Malays 2019;48(3):669–76. https://doi.org/10.17576/jsm-2019-4803-21.
[51] Topcu A, Darıcık F, Aydın K, Çelik S. Electrical properties of the carbon nanotube (CNT) reinforced composite plates for the PEM fuel cell bipolar plate application. In: 5th *international hydrogen technologies congress*. Turkey: Niğde; 2021. p. 221–3. IHTEC-2021), May 26-28.
[52] Hydrogen air MEA – 5 layer. https://www.fuelcellstore.com/fuel-cell-components/membrane-electrode-assembly/hydrogen-air-mea. [Accessed 28 September 2021].
[53] Zhu Y, Lin R, Jiang Z, Zhong D, Wang B, Shangguan W, Han L. Investigation on cold start of polymer electrolyte membrane fuel cells with different cathode serpentine flow fields. Int J Hydrogen Energy 2019;44:7505–17.
[54] Mawdsley JR, Carter JD, Wang X, Niyogi S, Fan CQ, Koc R. Composite-coated aluminum bipolar plates for PEM fuel cells. J Power Sources 2013;231:106–12. https://doi.org/10.1016/j.jpowsour.2012.12.074.
[55] Kumar S, Jayanarayanan K, Balachandran M. Thermal and mechanical behavior of functionalized MWCNT reinforced epoxy carbon fabric composites. Mater Today 2020;24:1157–66.
[56] Li M, Gu Y, Liu Y, Li Y, Zhang Z. Interfacial improvement of carbon fiber/epoxy composites using a simple process for depositing commercially functionalized carbon nanotubes on the fibers. Carbon 2013;52:109–21. https://doi.org/10.1016/j.carbon.2012.09.011.
[57] Fang C, Wang J, Zhang T. Interlaminar improvement of carbon fiber/epoxy composites via depositing mixture of carbon nanotubes and sizing agent. Appl Surf Sci 2014;321:1–9. https://doi.org/10.1016/j.apsusc.2014.09.170.
[58] Zakaria MR, Akil HM, Omar MF, Abdullah MMAB, Rahman AAA, Othman MBH. Improving flexural and dielectric properties of carbon fiber epoxy composite laminates reinforced with carbon nanotubes interlayer using electrospray deposition. Nanotechnol Rev 2020;9:1170–82. https://doi.org/10.1515/ntrev-2020-0090.
[59] Rodríguez-González JA, Rubio-González C, Meneses-Nochebuena CA, González-García P, Licea-Jiménez L. Enhanced interlaminar fracture toughness of unidirectional carbon fiber/epoxy composites modified with sprayed multi-walled carbon nanotubes. Compos Interfac 2017;24(9):883–96. https://doi.org/10.1080/09276440.2017.1302279.
[60] He Y, Yang S, Liu H, Shao Q, Chen Q, Lu C, Jiang Y, Liu C, Guo Z. Reinforced carbon fiber laminates with oriented carbon nanotube epoxy nanocomposites: magnetic field assisted alignment and cryogenic temperature mechanical properties. J Colloid Interface Sci 2018;517:40–51. https://doi.org/10.1016/j.jcis.2018.01.087.
[61] Rodríguez-González JA, Rubio-González C. Influence of sprayed multi-walled carbon nanotubes on mode I and mode II interlaminar fracture toughness of carbon fiber/epoxy composites. Adv Compos Mater 2019;28(1):19–36. https://doi.org/10.1080/09243046.2018.1458510.
[62] Yao X, Gao X, Jiang J, Xu C, Deng C, Wang J. Comparison of carbon nanotubes and graphene oxide coated carbon fiber for improving the interfacial properties of carbon fiber/epoxy composites. Compos B Eng 2018;132:170–7. https://doi.org/10.1016/j.compositesb.2017.09.012.
[63] T. Wilbeforce, O. Ijaodola, E. Ogungbemi, Z. El Hassan, J. Thompson, A.G. Olabi, Effect of bipolar plate materials on performance of fuel cells, Ref Modul Mater Sci Mater Eng 1-15. doi:10.1016/B978-0-12-803581-8.11272-X.
[64] Sharma K, Shukla M. Three-phase carbon fiber amine functionalized carbon nanotubes epoxy composite: processing, characterization, and multiscale modeling. J Nanomater 2014:837492 1–10. https://doi.org/10.1155/2014/837492.
[65] Shen Z, Bateman S, Wu DY, McMahon P, Dell'Olio M, Gotama J. The effects of carbon nanotubes on mechanical and thermal properties of woven glass fibre reinforced polyamide-6 nanocomposites. Compos Sci Technol 2009;69(2):239–44. https://doi.org/10.1016/j.compscitech.2008.10.017.
[66] Koçak NF, Topcu A, Aydın K, Çelik S, Topcu M. Experimental studies on flow fields of bipolar plate. Acad Persp Proc 2019;2(3):730–9. https://doi.org/10.33793/acperpro.02.03.80.